

Electronic Supplementary Information

Environmental Effects on Vibrational Properties of Carotenoids: Experiments and Calculations on Peridinin

Daniele Bovi,^a Alberto Mezzetti,^{*b,c} Rodolphe Vuilleumier,^d Marie-Pierre Gageot,^{e,f}
Bertrand Chazallon,^g Riccardo Spezia,^{*e} and Leonardo Guidoni^{*h,a}

Key words: carotenoids; Light Harvesting Complexes (LHC); Raman and InfraRed spectroscopy; Density Functional Theory (DFT); normal mode analysis; Quantum Mechanics / Molecular Mechanics (QM/MM)

Released on August 29, 2011

^a Dipartimento di Fisica, Università di Roma LA SAPIENZA, Rome, Italy.

^b LASIR UMR 8516, Université Lille I, France.

^c LPB, SB2SM, URA 2096, CEA-Saclay, France.

E-mail: alberto.mezzetti@cea.fr

^d Département de Chimie, Ecole Normale Supérieure, Paris, France and UPMC, Université Paris 06, France.

^e LAMBE UMR 8587 CNRS, Université d'Evry Val d'Essonne, France.

E-mail: riccardo.spezia@univ-evry.fr

^f Institut Universitaire de France (IUF), Paris, France.

^g PhLAM UMR 8523, Université Lille I, France.

^h Dipartimento di Chimica, Ingegneria Chimica e Materiali, Università de L'Aquila, Italy.

E-mail: leonardo.guidoni@univaq.it

Experimental details

Resonance Raman measurements were performed using an InVia Reflex spectroscope (Renishaw). This highly sensitive spectrometer is coupled to an Olympus BXFM free-space microscope. The excitation radiation ($\lambda = 514.5$ nm) is produced by an air-cooled Ar⁺ laser source (Modu-Laser, Stellar-pro). The laser power at sample was about 4 mW as measured by a Lasercheck power-meter (Coherent). The spectrometer configuration (250 mm focal length) provides a mean resolution of ~ 1.1 cm⁻¹/pixel which is reached with a holographic grating of 1800 grooves per mm and a Peltier-cooled front illuminated CCD detector (576x400 pixels). The microscope is equipped with an Olympus LWD 50x objective (0.5 N.A., 10.8 mm working distance) to provide a circular beam spot of diameter ~ 1 μ m. The confocal mode allows the nearly total elimination of the contribution of out of focus zone. The use of a microscope made possible to measure very small amounts of sample. Spectral positions were calibrated against the silicon line yielding a stable value of 520.4 ± 0.3 cm⁻¹. FT-Raman spectra were recorded with a Bruker IFS 66 V spectrometer. Radiation of 1064 nm from a Nd:YAG laser was used for the excitation with a laser power of 250 mW. The spectral resolution was set to 4 cm⁻¹. Spectra results from averaging of 10000-16000 scans, depending on the sample. Pure Peridinin spectra were obtained by subtraction of the spectrum of pure solvent from the spectrum of the solution. Fourier Transform Infrared spectra of solutions were recorded using a Thermo-Nicolet Magna 860 FTIR spectrometer using an attenuated total reflectance (ATR) device and a photovoltaic MCT detector. The FTIR spectrum of solid Peridinin was recorded using a Bruker Vertex 22 FTIR spectrometer equipped with an ATR device and a DTGS detector.

QM/MM description

The computational system was treated with different theories for different system partitions in a mixing approach based on QM/MM method. One Peridinin Model System molecule is described at DFT level and several solvent molecules with classical force field. The system partitioning is pictured in the sketch of Figure S1. The entire system (PMS + Solvent) is contained in the periodic classical box (*MD BOX*), wherein the quantum box (*QM BOX*) is defined. The *QM BOX* is not a real box (not introduce any barriers in the system), but it need have enclosed the area where the Plane-Wave basis set is expanded.

While the interactions between atoms belonging to the same model description (QM, or MM) are solved in the standard way for the respective method, the interactions involving both atoms, classical and quantum, are treated in multilayer approach (Fig. S1). For the first layer of classical atoms (defined as the classical atoms within $R_{NN} = 8.5$ Å cutoff from the quantum atoms) the Coulomb terms between the electronic density and the classical point charges are calculated without any approximation. In an intermediate region (between 8.5 and 19 Å) the interaction energy is calculated using dynamically generated restrained electrostatic potential (D-RESP) derived charges fitted on the electronic density¹. All the rest of the electrostatic interactions (including the periodic system images) is calculated using a multipolar expansion of the electron density.

In this approach, we have implemented three computational systems to produce QM/MM molecular dynamics, representative of the real peridinin solution at experimental condition (environmental temperature and atmospheric pressure). The three QM/MM systems (PMS and liquid solvent), referred hereafter as

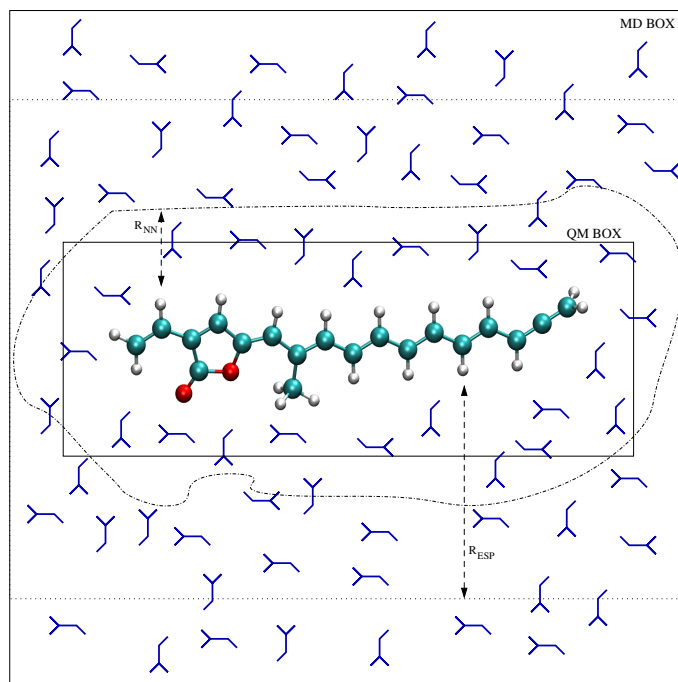


Figure S1 QM/MM system partitions.

MD-CHX (cyclohexane), MD-ACN (deuterated acetonitrile) and MD-MeOH (methanol) were performed adding to optimized structure of PMS several solvent molecules within periodic boundary conditions (440 CHX, 1749 ACN- d_3 and 3742 MeOH solvent molecules, respectively). Keeping the solute atoms fixed, solvent molecules and box sizes underwent a classical NPT pre-equilibration of about 2ns at 300K and 1 atm using the Berendsen² thermostat and barostat. Gromacs 4.0.7 package³ was used for this classical equilibration, obtaining three boxes of $41 \times 42 \times 47$, $59 \times 57 \times 71$ and $61 \times 58 \times 73 \text{ \AA}^3$ for CHX, ACN and MeOH respectively. We used a $17.0 \times 13.4 \times 28.4 \text{ \AA}^3$ box for the PWs representation of the QM part. From this starting point QM/MM simulations were performed using Born-Oppenheimer scheme for QM region using a time step of 0.36 fs. After an equilibration of 5 ps of NVT dynamics using the Nosé-Hoover thermostat⁴, the NVE production runs were propagated for about 12 ps for CHX and ACN and 17 ps for MeOH solutions.

Vibrations

The choice of the internal molecular variables is not in general straightforward, since a wrong set could lead to a fictitious convergence in which one part of the modes could be lost or misrepresented. Moreover for large systems (a few tenths of atoms) it is not evident how to choose a complete non-redundant basis set of internal variables. To this aim we used the Pulay's rules⁵ to define an appropriate basis set. They consist in bond stretching, angle combinations (symmetric and asymmetric deformation, rocking, scissoring, twisting and wagging), dihedral combinations and finally they add the molecular ring variables (ring deformation, puckering and torsion).

Gas Phase results

Table S1 Frequencies⁶ (cm⁻¹) calculated in harmonic approximation by hessian diagonalization of Peridinin and Peridinin Model System (PMS) in gas-phase and in different implicit solvents.

	Peridinin				PMS			
	Gas-Phase	CHX	ACN	MeOH	Gas-Phase	CHX	ACN	MeOH
$\nu_{C=C(7,11)}$	1504.33	1501.27	1493.66	1494.41	1507.99	1505.59	1496.59	1496.66
$\nu_{C=C(5,9,13)}$	1519.68	1516.64	1510.33	1510.37	1528.31	1525.22	1520.88	1521.04
$\nu_{C=C(1,3,11)}$	1548.19	1545.00	1537.69	1538.12	1548.49	1545.14	1537.76	1537.52
$\nu_{C=C(5,13)}$	1582.44	1580.42	1576.98	1576.83	1589.31	1587.29	1584.29	1584.56
$\nu_{C=C(7,11)}$	1589.99	1587.43	1583.52	1583.35	1596.33	1593.10	1591.40	1592.19
$\nu_{C=C(1,5,7,9,13)}$	1610.97	1609.26	1606.97	1606.68	1614.35	1611.34	1608.14	1608.46
$\nu_{C=C(1,5)}$	1632.70	1632.10	1631.55	1631.76	1633.48	1631.03	1628.93	1628.93
$\nu_{C=O(ester)}$	1757.69	1740.10	1708.89	1709.09	-	-	-	-
$\nu_{C=O(Lactone)}$	1772.44	1753.24	1711.23	1711.66	1779.05	1760.39	1716.50	1716.69
$\nu_{C=C=C_{asymm}}$	1937.16	1937.25	1935.81	1935.95	1964.91	1960.86	1951.32	1951.35

Table S2 Frequencies⁶ (cm⁻¹) calculated in harmonic approximation by hessian diagonalization of Peridinin and Peridinin Model System (PMS) in the gas-phase. IR and Raman intensities are labeled as high (h), medium (m) and low (l).

	Peridinin			PMS		
	Freq.	IR	Raman	Freq.	IR	Raman
$\nu_{C=C(7,11)}$	1504.33	m	h	1507.99	m	h
$\nu_{C=C(5,9,13)}$	1519.68	m	h	1528.31	l/m	h
$\nu_{C=C(1,3,11)}$	1548.19	l	h	1548.49	l	h
$\nu_{C=C(5,13)}$	1582.44	l/m	m	1589.31	l	h
$\nu_{C=C(7,11)}$	1589.99	l	h	1596.33	l	h
$\nu_{C=C(1,5,7,9,13)}$	1610.97	l	h	1614.35	l	h
$\nu_{C=C(1,5)}$	1632.70	m	h	1633.48	l	h
$\nu_{C=O(ester)}$	1757.69	m	l	-	-	-
$\nu_{C=O(Lactone)}$	1772.44	h	h	1779.05	h	l/h
$\nu_{C=C=C_{asymm}}$	1937.16	m	h	1964.91	m	h

QM/MM dynamics results

Table S3 Contribution (in %, from PED calculation⁷) of the different stretching motions ($v_{C=C_i}$) (numbering is the same as figures 1(b) and S2(a)) to the effective normal modes (Chain(j)) as obtained by QM/MM dynamics in different solvents. Only contributions larger than 5 % are shown for clarity.

CHX

Mode	$v_{C=C_1}$	$v_{C=C_3}$	$v_{C=C_5}$	$v_{C=C_7}$	$v_{C=C_9}$	$v_{C=C_{11}}$	$v_{C=C_{13}}$
Chain(1)		12.84		24.82			
Chain(2)					32.68		7.73
Chain(3)		25.71				13.32	
Chain(4)			9.32			22.62	
Chain(5)			7.82				22.71
Chain(6)			36.41		8.82		
Chain(7)	56.53						10.72

ACN

Mode	$v_{C=C_1}$	$v_{C=C_3}$	$v_{C=C_5}$	$v_{C=C_7}$	$v_{C=C_9}$	$v_{C=C_{11}}$	$v_{C=C_{13}}$
Chain(1)		23.59		12.76			
Chain(2)			5.09	4.25	34.01		12.20
Chain(3)	4.92	35.71					
Chain(4)				11.28		33.19	
Chain(5)			19.04				29.02
Chain(6)	24.16		10.07		10.85		7.03
Chain(7)	29.40		23.42				

MeOH

Mode	$v_{C=C_1}$	$v_{C=C_3}$	$v_{C=C_5}$	$v_{C=C_7}$	$v_{C=C_9}$	$v_{C=C_{11}}$	$v_{C=C_{13}}$
Chain(1)		16.36		21.26			
Chain(2)					30.51		13.56
Chain(3)		37.20		10.61			
Chain(4)						31.53	
Chain(5)	26.48		19.55		5.87		
Chain(6)					7.32		35.45
Chain(7)	31.09		23.15				

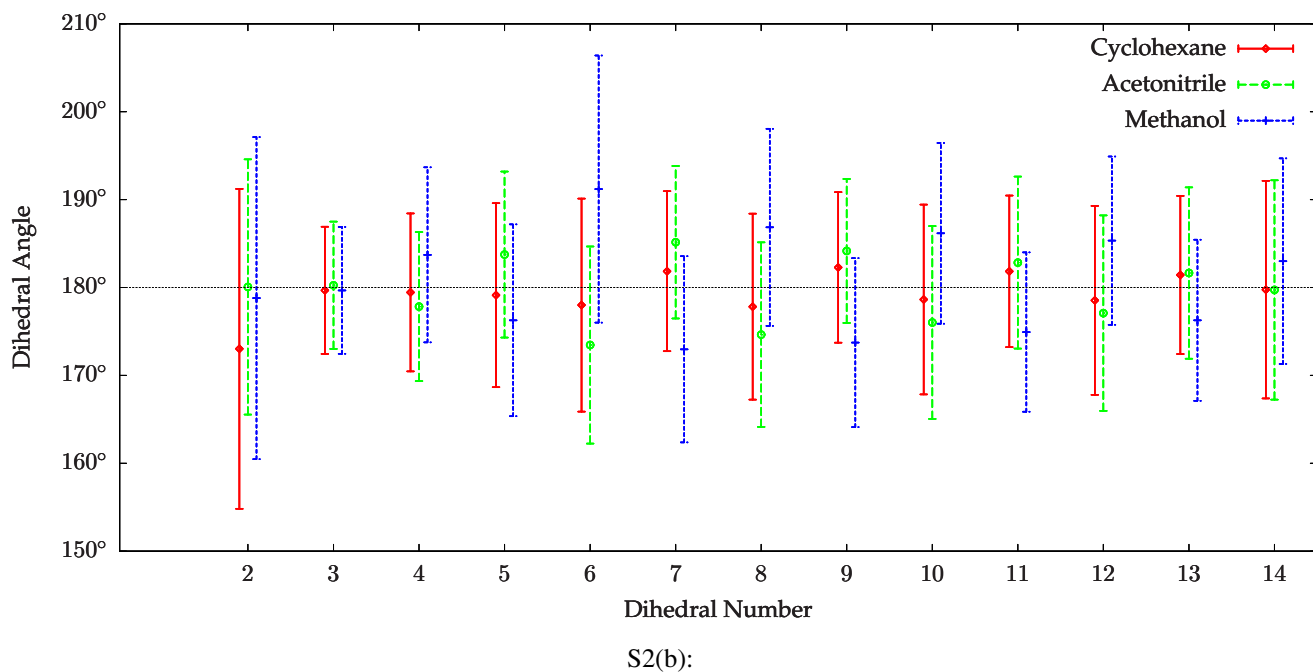
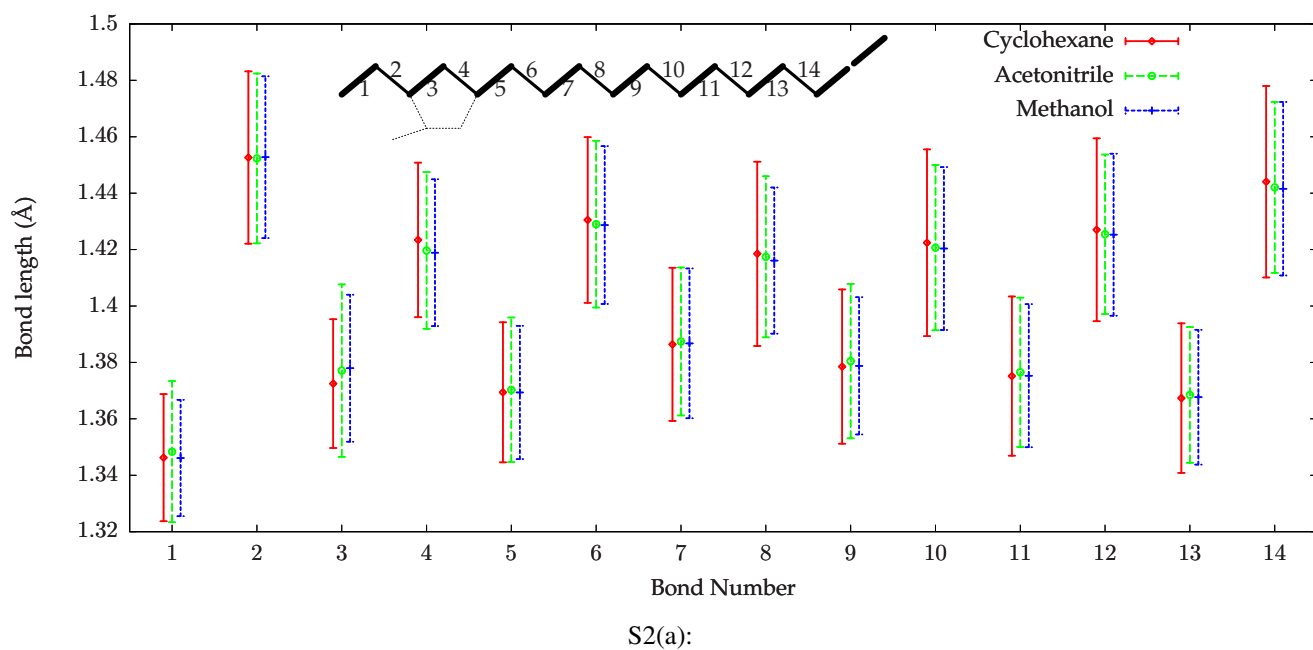


Figure S2 a) Average bond lengths of the polyene chain; Even bonds correspond to single C-C bonds and odd bonds to double C-C bonds (see sketch above). b) Average dihedral torsions of the Polyene chain; Referring to the sketch on the top, every number corresponds to the central bond of each dihedral angle. Mean values are obtained from equilibrated QM/MM molecular dynamics.

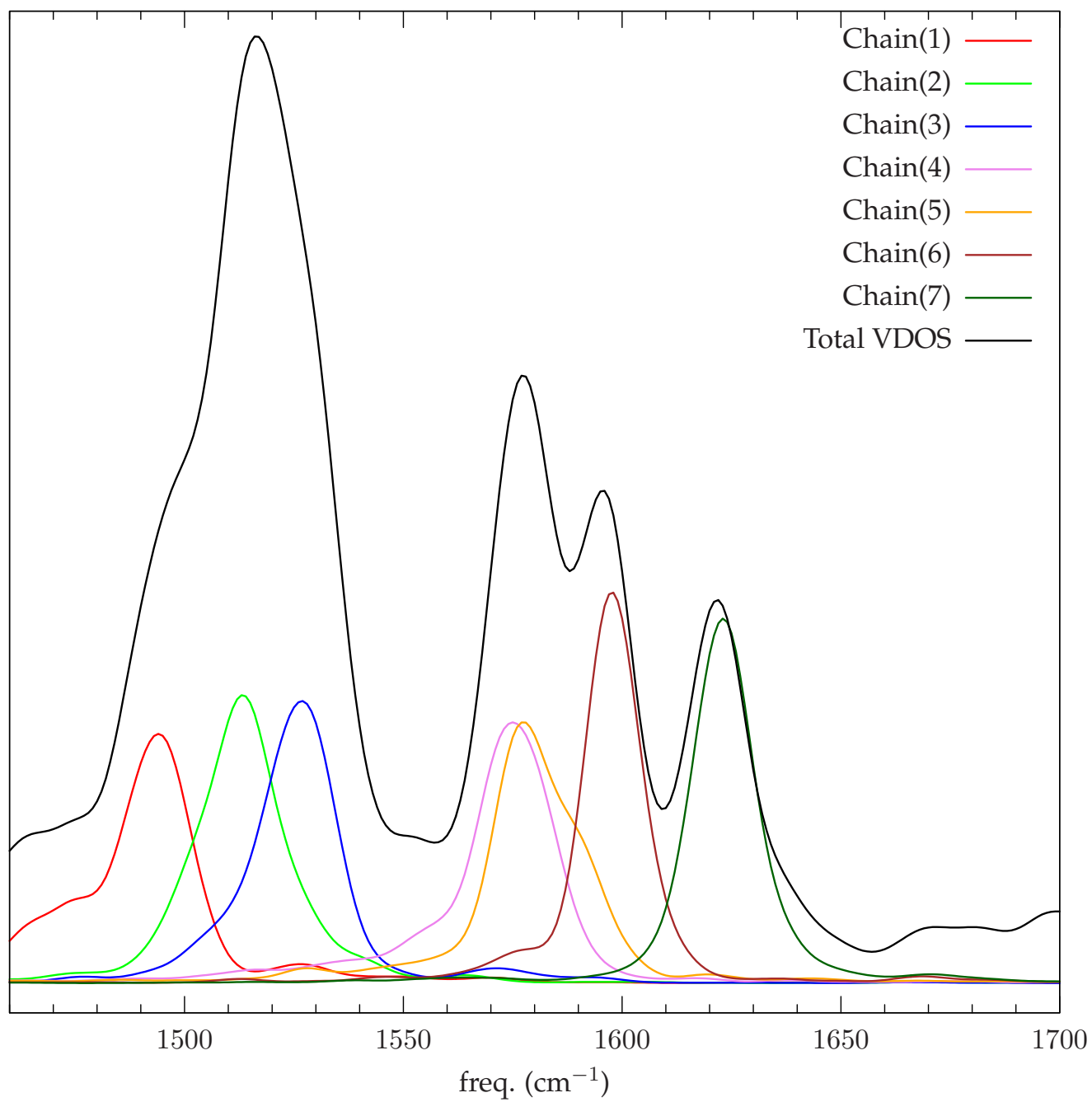


Figure S3 VDOS decomposition of the Polyene chain frequencies. The results shown here are obtained from PMS dynamics in ACN.

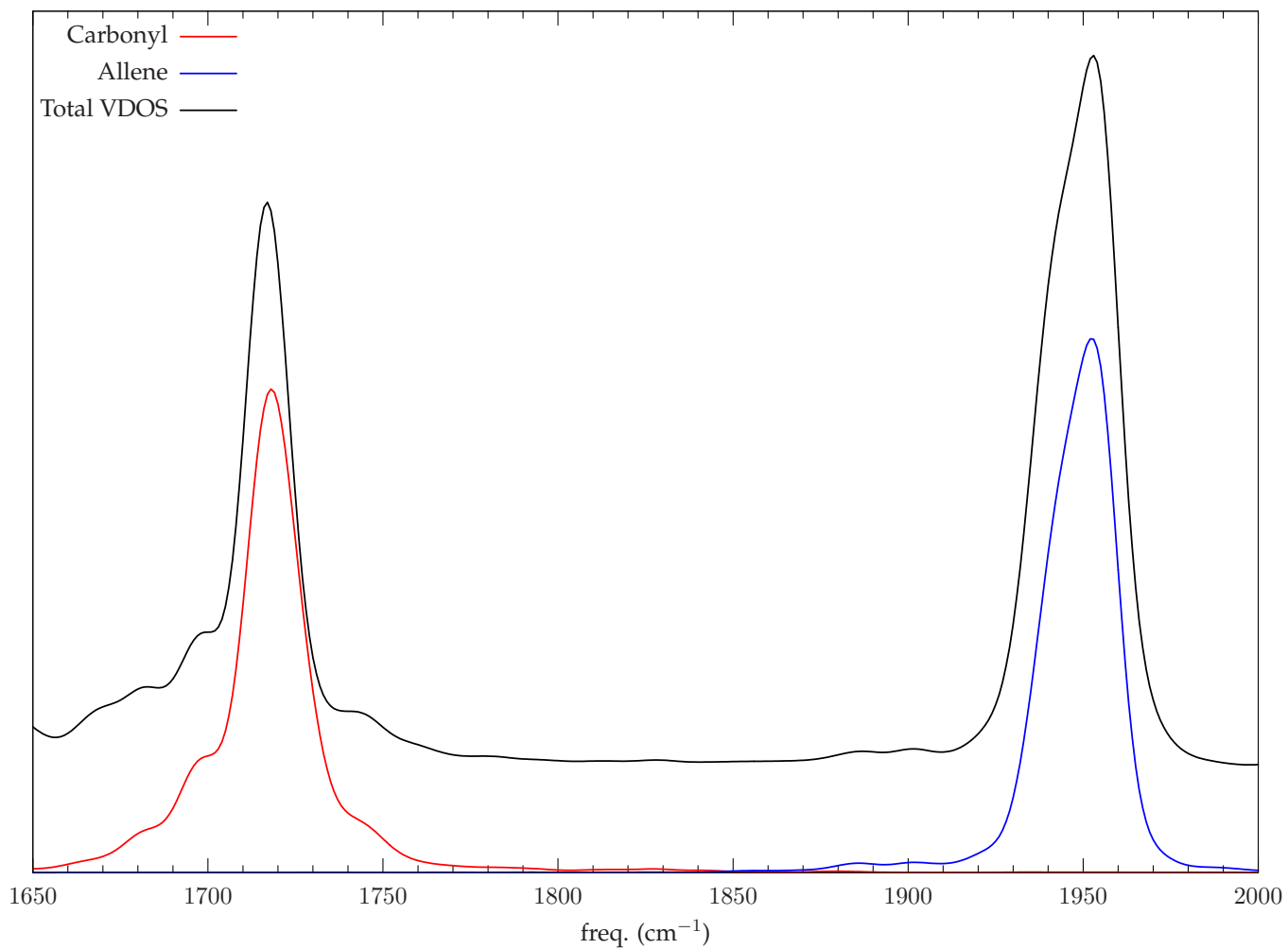


Figure S4 VDOS decomposition of the Carbonyl stretching and Allene antisymmetric stretching frequencies as obtained from ACN-MD simulation.

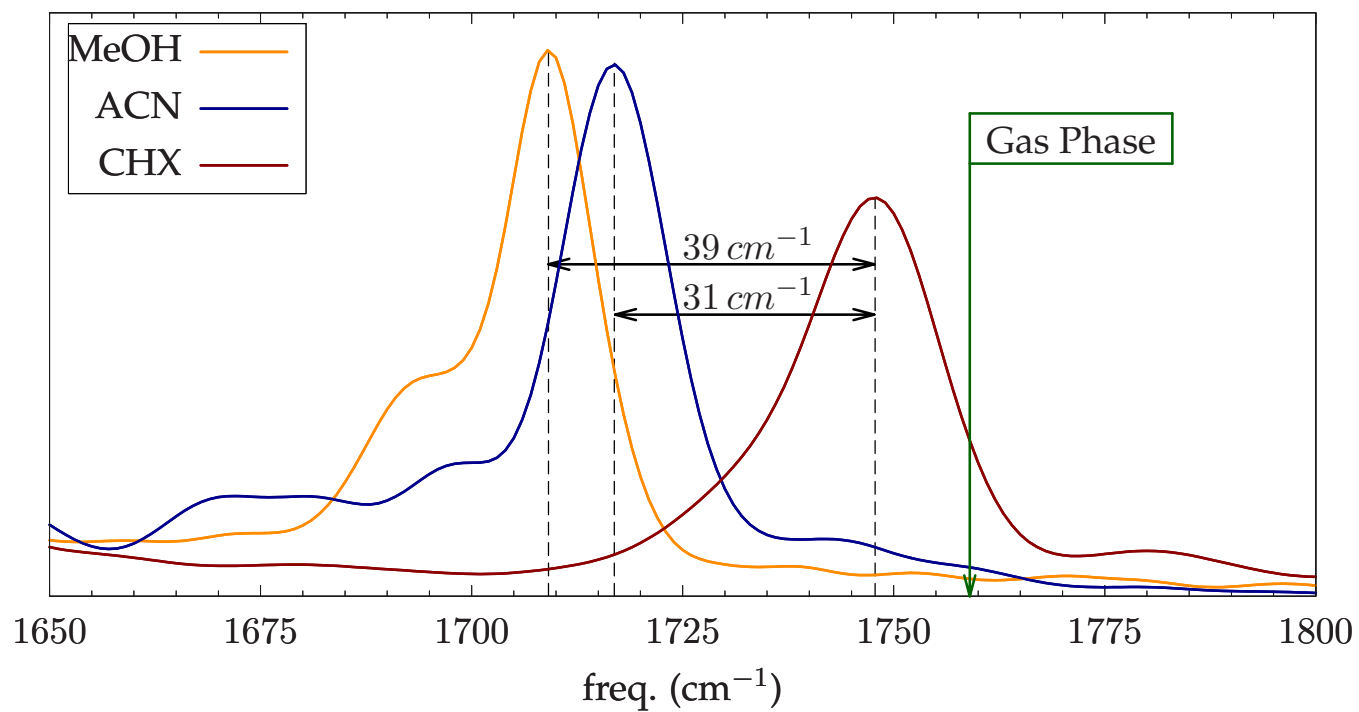


Figure S5 Total VDOS in the carbonyl frequencies range as obtained by MD simulations in different solvents.

Relevance to vibrational spectroscopy studies in PCP

Table S4 Lactonic C=O environments of peridinins in PCP X-ray cristal structure.

Per	H-bonds	C, N, O, S atoms within 3.8 Å	Polar groups within 5.0 Å	Notes
611	NO	CE1/PHE480 @ 3.5 Å CA/LYS124 @ 3.6 Å CB/ALA132 @ 3.8 Å	O/MET123 @ 4.4 Å	CHX-like
612	NO	CD/TYR122 @ 3.3 Å CE/MET123 @ 3.5 Å O/VAL119 @ 3.7 Å CG/VAL119 @ 3.6 Å	SD/MET123 @ 4.5 Å N/MET123 @ 4.6 Å	ACN-like
613	Possible	CE/TYR108 @ 3.5 Å C/CLA @ 3.6 Å	OH/TYR108 @ 4.7 Å	There is a large hole in correspondence to lactonic C=O and it is also directed toward the protein gate.
614	NO	CB/LYS143 @ 3.7 Å CG/VAL 146 @ 3.7 Å	N/LYS143 @ 4.6 Å O/LYS143 @ 4.8 Å	CHX-like; apolar atoms are packed around C=O similarly to CHX
621	NO	CA/PHE286 @ 3.4 Å CE/PHE180 @ 3.6 Å CB/PHE286 @ 3.7 Å N/PHE286 @ 3.7 Å	O/MET285 @ 4.3 Å	CHX-/ACN-like
622	NO	ND2/ASN284 @ 3.0 Å CB/ASN284 @ 3.5 Å CG/ASN284 @ 3.7 Å CE/MET285 @ 3.7 Å	O/ILE281 @ 4.0 Å OD1/ASN284 @ 4.9 Å O/SER280 @ 5.0 Å N/MET285 @ 4.9 Å	ACN-like
623	O(WAT) @ 2.8 Å	2C/CLA @ 3.6 & 3.7 Å	OH/TYR302 @ 4.4 Å OH/TYR270 @ 4.6 Å	MeOH-like; Tyr302 is H-bonded to water molecule that is H-bonded to C=O
624	NO	CB/LYS305 @ 3.7 Å CB/VAL308 @ 3.7 Å CG2/VAL308 @ 3.6 Å	O/LYS305 @ 4.8 Å N/LYS305 @ 4.6 Å	CHX-like

References

1. A. Laio, J. VandeVondele and U. Rothlisberger, *J. Phys. Chem. B*, 2002, **106**, 7300–7307.
2. H. J. C. Berendsen, J. P. M. Postma, W. F. van Gunsteren, A. Di Nola and J. R. Haak, *J. Chem. Phys.*, 1984, **81**, 3684.
3. Berendsen, D. v. Spoel and R. van Drunen, *Comput. Phys. Commun.*, 1995, **91**, 43–56.
4. W. Hoover, A. Ladd and B. Moran, *Phys. Rev. Lett.*, 1982, **48**, 1818–1820.
5. P. Pulay, G. Fogarasi, F. Pang and J. Boggs, *J. Am. Chem. Soc.*, 1979, **101**, 2550–2560.
6. These frequencies are obtained at PBE level and no scaling factor is considered, as also done in our previous work⁸. Since they are used in this work only to show differences between Per and PMS (see tabs S1 and S2) and differences exclusively due to polarization effects by homogeneous electric field (tab. S1).
7. M.-P. Gaigeot, M. Martinez and R. Vuilleumier, *Mol. Phys.*, 2007, **105**, 2857–2878.
8. A. Mezzetti and R. Spezia, *Spectroscopy*, 2008, **22**, 235–250.